CHAPTER 3

Chapter 3

Determination of Structure and Immunological Function of the Exopolysaccharide Synthesized by *Klebsiella pneumoniae* PB12

3.1. Introduction

Klebsiella pneumoniae, a Gram-negative opportunistic pathogen causes hospital-acquired urinary tract infections, respiratory tract infections, and septicaemias (Podschun & Ullmann, 1998). A common feature shown by *K. pneumoniae* strains is its ability to form biofilm which provides shelter and homoeostasis to the cell population under its cover. Biofilm comprised of extracellular polymeric substance (EPSs) which has the potential to prevent the influx of certain antimicrobial agents (Gilbert et al., 1997). EPSs possess metal binding property and can seize toxic metal ions to protect bacterial cells (Wolfaardt et al., 1999). EPS also renders a major virulence factor contributing towards expression of diseases (NIH, 2002). The chemical composition of EPSs differs widely depending on the microorganism. EPSs are generally composed of glycoprotein, polysaccharide, protein, cellulose, lipid, glycolipid and nucleic acid (Branda et al., 2005). The major structural component of EPSs is polysaccharide which is either neutral or polyanionic in nature. The anionic nature is due to the presence of uronic acids which is thought to improve the binding ability of bivalent cations and enhance the mechanical strength of the EPSs (Davey & O'Toole, 2000). Bacterial exopolysaccharides have also shown biological activities like anti-tumor and immunomodulatory properties that significantly varied with the degree of branching, molecular mass, conformation and

chemical modification (Sen et al., 2014). Some species of the genus *Klebsiella* were reported earlier to produce exopolysaccharides in culture medium. Fucogel, a polysaccharide produced by *Klebsiella pneumoniae* I-1507 was found to compose of galactose, 4-*O*-acetyl-galacturonic acid and fucose (Guetta et al., 2003). In a separate study, Rättö et al. (2001) isolated galacturonic acid containing heteropolysaccharide from two *K. Pneumoniae* strains. Bales et al. (2013) characterized another EPSs isolated from *K. pneumoniae* which was found to comprise of 1.3 % glucose, 49.4 % mannose, and 5.0% GlcA. In general, polysaccharides activate macrophages, T-helper, NK, and other effector cells and thereby activate various chemokines, cytokines (IL-2, IL-6, IL-10, TNF-α, and IL-12) and interferon (IFN-γ) resulting stimulation of host's immune system (Yu et al., 2014). Earlier study has shown that the capsular polysaccharide of pyrogenic liver abscess (PLA) *K. pneumoniae* induces secretion of tumor necrosis factor-α (TNF-α) and interleukin-6 (IL-6) by macrophages through Toll-like receptor 4 (TLR4) (Yang et al., 2011). In another study Hsieh et al. established the role of virulence of O1 antigen obtained from PLA-associated *K. pneumoniae* (Hsieh et al., 2012). It was proposed by earlier authors that EPS of *K. pneumoniae* have infection-enhancing capabilities by hindering the acid phosphatase release from the lysosomal fraction of peritoneal macrophages (Straus et al., 1985). It was shown earlier that trace amount of *K. pneumoniae* extracellular capsular polysaccharide inhibited macrophage maturation and function (Yokochi et al. 1977). The details of the structural characterization of the exopolysaccharide isolated from *Klebsiella pneumoniae* PB12 along with the investigations of biological activities are reported in this chapter.

3.1.1. Parameters effecting EPS production

3.1.1.1. Nutrient concentration

The concentration of nutrient has a significant effect on EPS production and composition. Medium containing excess of glucose has been shown to increase the production of EPS (Flemming & Wingender, 2001). Earlier report showed that a variety of nitrogen sources including ammonium, nitrate, nitrite, and amino acids can be utilized by bacteria for EPS synthesis (Sutherland, 1990a; Amarger, 2001). Among these, ammonium salts and amino acids are the most common ones (Sutherland, 1990a). Depending upon the nitrogen substrate utilized, the yield of EPS varied (Datta & Basu, 1999). Low nitrogen content in the growth medium also influences the EPS production (Sleytr, 1997). Under nitrogen limited condition in the medium, 60% of the glucose was converted into exopolysaccharides in some species of *Aureobasidium*, *Sinorhizobium*, *Escherichia* and *Pseudomonas* (Lee et al., 1999; Sutherland, 2001). Whereas, increase in nitrogen content (ammonium salts) in the medium provokes microbes like *Pseudomonas* sp. and *Rhodococcus* sp. to produce extracellular protein (Sanin et al., 2003).

3.1.1.2. Growth phase

The production of EPS varies with growth phase in different genera. In few strains of *Pseudomonas aeruginosa* and *Staphylococcus epidermidis*, the production of EPS has been observed during late logarithmic and early stationary phase of growth (Sutherland, 2001). In many bacterial species, growth and EPS production occur concurrently (Datta & Basu, 1999). In some species maximum EPS production occurs in

the exponential phase (Bramhachari & Dubey, 2006), while in others, EPS production is maximized in the stationary phase (Datta & Basu, 1999).

3.1.1.3. pH and temperature of the cultivation medium

The pH of the culture medium has an intense effect on the EPS production. Studies have shown that the extremes of pH of the medium (pH 2.0-3.0 or pH 10) resulted in inhibition of microbial growth as well as the biosynthesis of extracellular polymers (Stredansky & Conti, 1999). In *Antrodia camphorate*, the pH of the medium was found to have stimulatory effect on EPS production. Shu and lung (2004) reported that the maximum EPS production in *Antrodia camphorates* occured at pH 5.0. They also proposed that the pH profiles of the culture medium also influence molecular mass of the EPS compounds. The effect of the cultivation temperature on the EPS biosynthesis has been investigated by many authors. In general, the optimal cultivation temperature for the production of the majority of EPS molecules was projected between 26 and 31 °C (Lory, 1992). However, in certain cases low temperature was found to be more favorable for EPS production as reported in *Listeria*. It was observed earlier that in *Listeria monocytogenes* cells, a cultivation temperature of 10 °C induces the production of extracellular cold shock protein (Briandet et al., 1999).

3.1.2. Various methods for extraction and characterization of EPS

3.1.2.1. Extraction of EPS

It is important to adopt a method where no or minimal cell lysis or disruption or alteration of the EPS occurs while extracting it from the bulk of extracellular biopolymeric substances. Several physical, chemical or combined methods have been proposed to extract EPS from cells from different sources (e.g. biofilm, sludge and cell suspension) such as the high-speed centrifugation, heating, ultrasonication. Physical extraction includes centrifugation, ultrasonication and heating. Whereas, common chemical extraction includes uses of NaOH, ethylenediamine tetraacetic acid (EDTA) and cation exchange resin.

3.1.2.2. Characterization of EPS

3.1.2.2.1. Colorimetric analyses

It is known that the EPS is often associated with other complex extracellular polymeric like substances Colorimetric analyses can be made to quantify these components contaminated with EPS. The carbohydrate content is usually measured by the phenol–sulfuric acid method (York et al., 1985). The protein content can be quantified by using the method described previously (Bradford, 1976). The uronic acid content of the EPS can be measured by using carbazole-sulfuric acid reaction (Chaplin & Kennedy, 1986). For quantification of nucleic acid content of the EPS, various methods have been used such as DAPI fluorescence method (Frolund et al., 1996), diphenylamine method (Liu & Fang, 2002), or the UV absorbance method (Boonaert et al., 2001).

3.1.2.2.2. A) Chemical methods

3.1.2.2.2.1. Estimation of total carbohydrate

Total carbohydrate content of polysaccharide was estimated using phenol–sulfuric acid method (York et al., 1985). A 1000 μg solution of sample was prepared by 5 mg sample in 5 ml distilled water and two other concentrations, 100 μg and 80 μg from that solution were prepared. Standard glucose solution of different concentrations (20 μg, 40 μg, 80 μg, 100 μg and 200 μg) were prepared. Then, 1 ml of each standard glucose solution was taken into five test tubes. 1 ml of each solution of sample was pipette out into two test tubes while 1 ml water taken into a test tube served the blank test. After that 1 ml of 5% phenol solution and then followed by 5 ml of concentrated sulfuric acid (H_2SO_4) were added into each test tube. All the tubes were shaken very well and kept for 15 min at ambient temperature. Finally, absorptions of each solution were recorded at 490 nm in Shimadzu UV-visible spectrophotometer, model 1601. Concentrations of standard solution were plotted against absorption in a graph to obtain standard curve. From absorption values of the sample solution, exact carbohydrate percentage of the sample was estimated with the aid of the standard curve.

3.1.2.2.2.2. Monosaccharide composition

The monosaccharide composition with their absolute configurations is needed to determine the complete structure of polysaccharide. The polysaccharide was hydrolyzed with trifluroacetic acid (TFA) [CF_3COOH] (2M) to obtain monosaccharide constituents. Sugar composition was identified by chromatographic studies with the hydrolyzed

product. Solution of strong acids such as sulfuric, hydrochloric or TFA can be used in acid hydrolysis. In the present work, TFA had been used to degrade polysaccharide (glycosidic linkages) due to its volatility. Then monosaccharides were converted into alditols by $NaBH_4$ reduction followed by acetylation to increase the volatility. The derivatives were identified from retention times compared to standards by GLC. The overall reaction scheme has been presented below (Scheme 3.1).

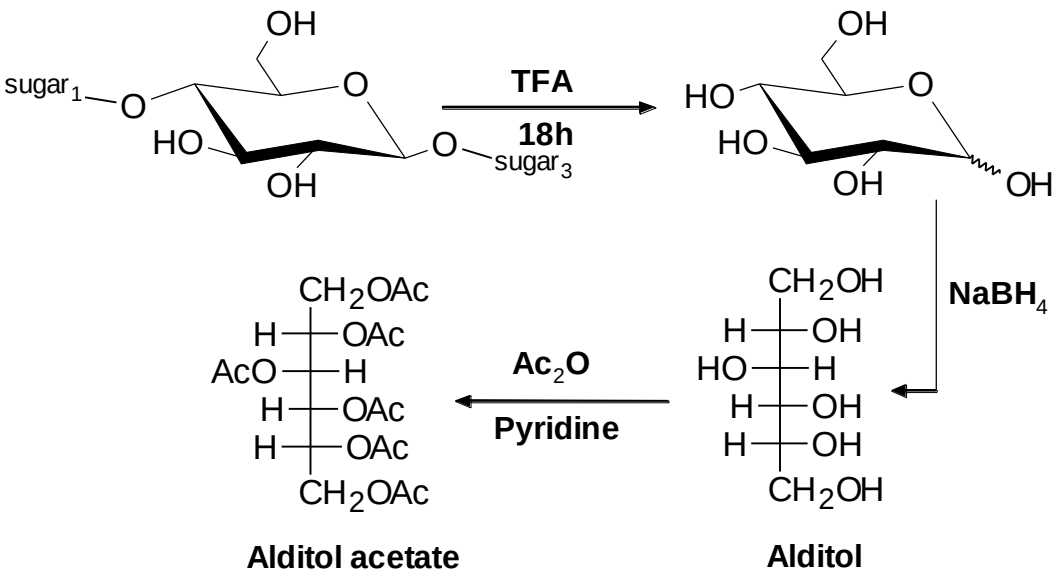

Scheme 3.1.

Uronic acids (its derivatives) are resistant to normal acid catalyzed hydrolysis due to the inductive effect of the carboxyl group (BeMiller JN, 1967). So in the present case (reaction strategy shown below; Scheme 3.2) carboxyl-methyl reduced polysaccharide (Maness et al., 1990) on hydrolysis followed by GLC examination of the corresponding alditol acetates provided the identification of the sugar residues.

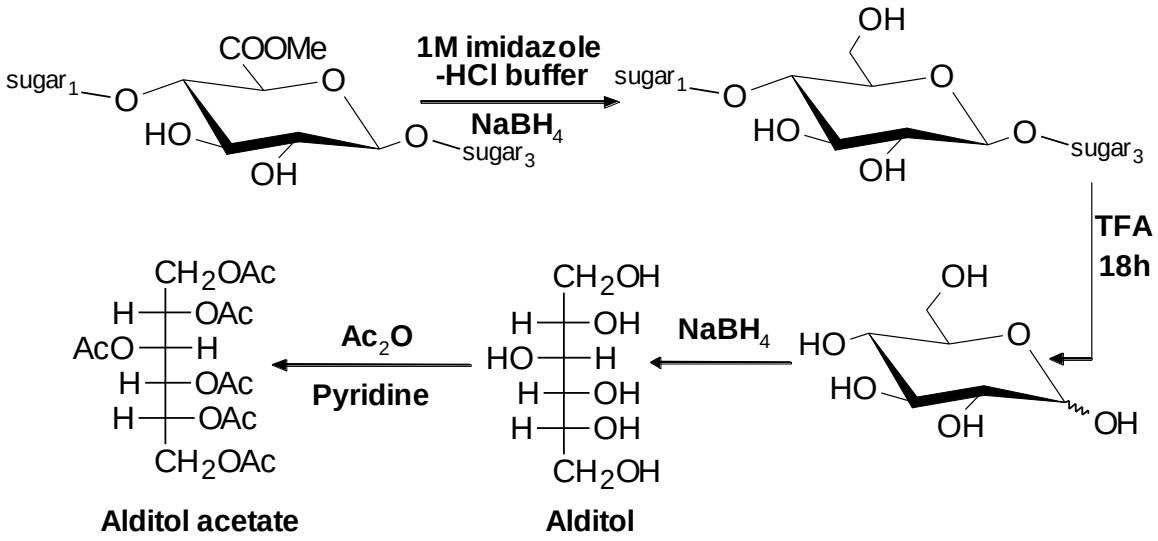

Scheme 3.2.

Sugars have either D or L configuration. To determine their absolute configurations, monosaccharides were subjected to acid catalyzed reaction with optically active 2-butanol or 2-octanol. The glycosides obtained were then trimethylsilylated or acetylated and analyzed by GLC. The diastereomers obtained from the D and L isomers had different GLC retention times and can be distinguished with the help of authentic standards (Gerwig et al., 1978).

3.1.2.2.2.3. Preparation of alditol acetates

The polysaccharide was hydrolyzed with TFA. The mixture of sugars in water was reduced by treating with sodium borohydride at room temperature for 4 hours. Excess $NaBH_4$ was destroyed by acidification with acetic acid and the free boric acid was removed as methyl borate by co-distillation with MeOH. The alditols were dried and then

acetylated by heating with (Ac_2O)-pyridine (1:1) mixture at 100ºC for 1 hour. The material was taken up in $CHCl_3$ for injecting into GLC (Bjorndal et al., 1967).

3.1.2.2.2.4. Determination of absolute configuration of monosaccharide

The absolute configurations of sugar residues were determined by the method based on Gerwig et.al. (1978). After trifluoro acetic acid hydrolysis, the polysaccharide (1.5 mg) was treated with (+)-2-butanol (in 250 µl of 0.625 M HCl) and Per-*O*-TMS-derivatives were prepared with N,O-bis (trimethylsilyl) trifluoro acetamide (BSTFA). The products were analyzed by GLC using a capillary column (SPB-1, 30 m x 0.26 mm) with a temperature program (3 ºC min^{-1}) from 150-210 ºC. The (+)-2-butyl 2,3,4,6-tetra–*O*-TMS-glycosides obtained were identified by comparison with those prepared from the D and L enantiomers of the monosaccharides.

3.1.2.2.2.5. Linkage analysis

Methylation analysis is a well-known chemical method for determination of the linkage position of sugar residues present in polysaccharide. Although this information can be obtained non-destructively by nuclear magnetic resonance (NMR) spectroscopy, methylation analysis is still a powerful method in carbohydrate structural analysis (Ciucanu & Kerek, 1984) alone or in combination with NMR spectroscopy.

The derivetization of polysaccharide for methylation analysis involves conversion of all free hydroxyl groups into methoxy group. Then acid hydrolysis breaks only the interglycosidic linkages leaving the methyl ether bonds intact. The hydrolyzed monomers

are then reduced, followed by acetylation to produce volatile partially methylated alditol acetates (PMAA).

The substitution pattern of the *O*-acetyl group of the PMAA indicates the linkage patterns of the corresponding sugars in the polysaccharide. PMAA (Sweet et al., 1975) are separated and identified through GLC. On a specific column the retention times of PMAAs is highly reproducible. Relative retention times (generally with respect to 1,5-di-O-acetyl-2,3,4,6-tetra-O-methyl-D-glucitol) are used in the literature. The comparison with literature values should only be made with the same column run under the same condition. When methyl esters of galacturonic acid are present as a monomer unit in polysaccharide, carboxy methyl reduced polysaccharide (Maness et al., 1990) is used for methylation. The methylated $LiAlH_4$ reduced polysaccharide (Abdel-Akher & Smith, 1950) is also used.

3.1.2.2.2.6. Methylation analysis: Ciucanu and Kerek method

In the present thesis the polysaccharides were methylated according to the methods described by Ciucanu & Kerek (1984). The polysaccharide (3-5 mg) was kept overnight on phosphorous pentoxide (P_2O_5) in a vacuum decicator and dissolved in 0.5 ml of distilled DMSO. Solid finely grounded NaOH dust was added and stirring for 30 min. Then 0.5-1 ml CH_3I was added and stirred for 1-1.5 h. The methylated material was isolated by partition between $CHCl_3$ and H_2O (5:2, v/v). The $CHCl_3$ solution of methylated product was dried on water bath to yield solid product. The methylated sugar was then hydrolyzed with formic acid (HCOOH) for 1 h and the excess acid was removed by co-distillation with water (Scheme 3.3). The hydrolyzed methylated products

were acetylated by Ac_2O-pyridine (1:1) mixture at 100 ºC for 1 h. The alditol acetates of methylated sugars were identified by GLC (using column A and column B) and GLC-MS (using HP-5 fused silica capillary column).

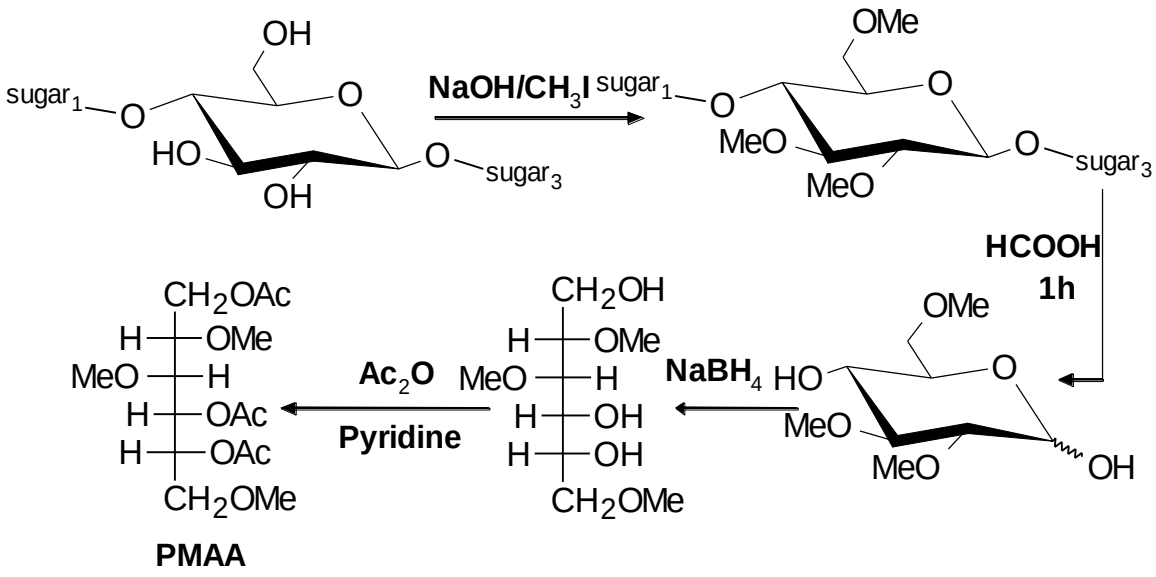

Scheme 3.3.

3.1.2.2.2.7. Periodate oxidation

Polysaccharides are susceptible towards the reaction with oxidizing agents such as periodic acid or its salts due to the presence of free hydroxyl groups. Non-terminal units e.g. (1→2) and (1→4)-linked hexopyranose units consume one equivalent of periodate per mole yielding dialdehydes. Whereas, (1→3)-linked hexopyranose unit or branched at C-2 or C-4 positions will not be affected by this reaction due to absence of adjacent–OH groups. The products of the periodate oxidation reaction are methylated, followed by reduction and conversion to alditol acetates. PMAA are then identified by GLC and GLC-MS. The partially methylated alditol acetates corresponding to hexopyranose

moieties that contain (1→3)-linkage or branched at C-2 or C-4 positions will survive in the native polysaccharide after this reaction. So the periodate oxidation study further supports the linkages of sugar units as determined by methylation experiments.

In the present chapter polysaccharide was treated with sodium metaperiodate and mixture was kept 48 h in the dark at 4ºC. The excess periodate was destroyed by ethylene glycol and the solution was dialyzed against distilled water and dried. A portion of the dried product was reduced with $NaBH_4$ and neutralized with AcOH. The resulting material was obtained by co-distillation with MeOH. Then the product was hydrolyzed by 2M TFA for 18 h at 100 ºC and the alditol acetates were prepared as usual. Another portion was methylated by the method of Ciucanu & Kerek (1984) and the alditol acetate of this methylated product was prepared for GLC and GLC-MS analysis.

In case of polysaccharide containing methyl ester of galacturonic acid, then periodate-oxidized, $LiAlH_4$-reduced polysaccharide was mixed with 0.5 M CF_3COOH and allowed to stand for 48 h at room temperature. The acid was removed and the hydrolyzed material was analyzed by GLC after conversion to alditol acetates.

3.1.2.2.2.8. Smith degradation

Oligosaccharides (OS) are more easily characterized than polysaccharide (PS) with the help of NMR spectroscopy. Smith degradation is another method to degrade PS to OS or modified PS. This method is utilized to simplify the identification of the repeating unit by selective removal of some of the residue. The oxidation yields a product in which vicinal hydroxyl groups have been oxidized to aldehydes by cleavage of carbon-

carbon bonds. $NaIO_4$ does not affect residues with out any vicinal hydroxyl groups. The reduction of aldehyde yields a polyalcohol. On mild acidic hydrolysis, these yield OS or modified PS that contains sugar residues and fragments have modified sugar residue.

3.1.2.2.3. B) Analytical methods

3.1.2.2.3.1. Gas liquid chromatography

Chromatography is a non-destructive method for resolving a mixture of components into individual components through equilibrium distribution between two phases. Gas-liquid chromatography consists of a mobile gas phase and a stationary liquid phase that is coated on to either a solid matrix (e.g. diatomaceous earth) or the wall of a capillary tube. Stationary phase has a sufficiently low vapour pressure at the column temperature. So that it can be considered as non-volatile. The sample mixture in gaseous form is run through the column with a carrier gas (e.g. N_2). Separation can be achieved by the differences in the distribution ratios of the components of the sample between the mobile (gaseous) and stationary (liquid) phases causing them to move through the column at different rates and with different retention times. After elution, the components can be detected by a suitable detector.

For GLC (Bjorndal et al., 1967) separation, sample must be volatile. As monosaccharides are not volatile, there must be derivetized into their alditol acetates. The essential part of the derivetization procedure (Southgate, 1976) is the reduction of neutral sugars to alditol and subsequent acetylation. The alditol acetates are dissolved in suitable solvents such as chloroform or methylene chloride and injected into a GLC column.

In this work two types of columns: 3% ECNSSM (a nitrile-silicon polyester copolymer) and 1% OV-225 (a silicon polymer containing methyl, phenyl and nitrile groups) have been used. For detection the flame ionization detector was used. The detector responds to all organic compounds except formic acid, the response being greatest for hydrocarbons.

3.1.2.2.3.2. Gas liquid chromatography-Mass spectrometry

Mass spectrometry coupled with gas chromatography has been reported to be a very useful tool in biological and chemical studies. GLC-MS (Bjorndal et al., 1967) analysis of carbohydrate has advantages because it is very sensitive and a small amount of sample is required. In GLC-MS, volatile molecules are identified by their GLC-retention times and by their mass spectra. GLC-MS is used to analyze the monosaccharide composition obtained from different degradation methods e.g. the alditol acetates, the partially methylated alditol acetates (PMAA). The electron impact fragmentation pattern of the mass spectra of PMAA is well documented for all linkage patterns of all known sugars.

3.1.2.2.3.3. Nuclear Magnetic Resonance (NMR) Spectroscopy

Nuclear Magnetic Resonance (NMR) is the most powerful and non-destructive technique for identification of monosaccharide composition, elucidation of α or β anomeric configurations, linkage patterns and sequence of sugar units in the repeating unit of the polysaccharide. Different types of 1D (^{1}H, ^{13}C) and 2D (COSY, DQF-COSY,

TOCSY, NOESY, ROESY, HMQC and HMBC) NMR techniques are adapted to characterize the structure of a polysaccharide.

3.1.2.2.3.4. One-dimensitional NMR

Two types of 1D NMR spectroscopy in common use today are ^{1}H (proton NMR) and ^{13}C (carbon-13 NMR). The sample was kept over P_2O_5 in vacuum to remove water and deuterium exchanged by lyophilization with D_2O. The signal for residual HOD was suppressed. The protons of polysaccharide show chemical shifts in the range of 1.0-6.0 ppm. The anomeric proton region is found in the range of 4.4-5.5 ppm. The remaining rings protons resonate in the range of 3.0-4.2 ppm. Signal of acetyl methyl proton appears at 2.0-2.2 ppm. Normally, the α-anomer resonates downfield compared to the β-anomer in D-pyranoses. From coupling constant $^{3}J_{H1,H2}$, the anomeric configuration of a glucopyranosyl residue can be determined. If $^{3}J_{H1,H2}$ is nearly 3-4 Hz, the anomeric configuration of this residue is α. On the other hand, the configuration will be β if that value is nearly 7-10 Hz. $J_{H1,H2}$ values are not always sufficient to determine the anomeric configuration of the sugars. If the glycosyl residue has the manno configuration, the distinction between the α and β anomer is very difficult as the coupling constant values for α ($J_{H1,H2}$ ~ 1.8 Hz.) and β ($J_{H1,H2}$ ~ 1.5 Hz.) are too close.

The one bond ^{13}C-^{1}H couplings constant are useful for the determination of anomeric configuration of sugar residues (Bock et al., 1982) For D sugars 1JC1,H1 ~ 170 Hz indicates an α-anomeric configuration whereas 1JC1,H1 ~160 Hz indicates a β-anomeric configuration (Bock & Pedersen, 1974) which is reversed for the L sugars.

In the ^{13}C NMR spectra, anomeric carbon signals lie in the region 90-110 ppm whereas non-anomeric carbons in 60-90 ppm. The α-anomeric carbon signals appear generally in the range of 95-103 ppm whereas most of the β-anomeric carbons appear in the region of 101-105 ppm. In case of methoxy sugar, the methyl carbons appear in the region 55-61 ppm. Acetyl methyl carbon appears in the region 18-22 ppm. Signals for carbonyl carbons are generally observed in the range of 165-185 ppm. Unsubstituted ring carbons usually have the chemical shifts between 65 ppm and 75 ppm (Agarwal, 1992). If there is any linkage at any carbon, the signal for that carbon will suffer a downfield shift by 4-10 ppm and the carbon next to that one will appear in a little upfield region (by 0.7-4.7 ppm) (Agarwal, 1992).

3.1.2.2.3.5. Two-dimensional NMR

A conventional ^{1}H NMR spectrum has a frequency axis and an intensity axis; Two-dimensional (2D)- NMR spectra have two frequency axes and one intensity axis. 2D-NMR can be applied to analyze complex spectra, which are difficult to predict by conventional methods (Kalsi, 2004). In present work different 2D-NMR experiments such as DQF-COSY (Double quantum filtered correlation spectroscopy), TOCSY (Total correlation spectroscopy), NOESY (Nuclear overhauser enhancement spectroscopy), ROESY (Rotating frame overhauser enhancement spectroscopy), HMQC (Heteronuclear multiple quantum coherence) and HMBC (Heteromultiple bond coherence spectroscopy) have been used.

COSY (Correlation spectroscopy) identifies pairs of protons, which are coupled to each other. COSY or DQF-COSY gives information about the protons of an individual

sugar residue through a three-bond coupling. It is a ^{1}H homonuclear shift correlation spectrum that provides information on spin coupling networks with in a residue through the observation of the cross peaks off diagonal.

A TOCSY spectrum correlates protons that are in the same spin system and gives both short range and long-range correlations. It is useful in the identification of individual monosaccharide residue.

The NOESY spectrum provides information on through space rather than through bond couplings. NOE connectivities are often observed between the anomeric protons of a particular sugar residue to protons of another sugar residue that is glycosidically linked to the former. NOESY experiments give information on linkages and sequence of sugar residues in a polysaccharide.

ROESY is used to determine signals arisen from protons, which are close in space but not closely connected by chemical bonds. A ROESY spectrum yields through space correlations via the Rotational nuclear overhauser effect (ROE). ROESY is especially useful for cases where NOESY signals are weak because they are near the transition between negative and positive. ROESY cross peaks are always negative. The ROESY experiment also yields cross peaks arisen from chemical exchange.

In a heteronuclear spectrum like HMQC NMR spectrum, all signals in the spectra represent a direct correlation between a carbon and a proton.

An HMBC experiment gives long range coupling between proton and carbon (two or three bonds) with high sensitivity. HMBC experiments establish multiple-bond

correlation through the glycosidic bonds and this together with NOESY experiments gives necessary information on linkages and sequence of sugar residues in a polysaccharide.

3.1.2.2.4.. Physical methods

3.1.2.2.4.1. SEM and Energy dispersive X-ray study (*EDS)*

SEM is commonly used for studying the surface morphology of cells and other biomaterials. The technique makes use of a primary beam of electrons that interact with the specimen of interest, in a vacuum environment, resulting in different types of electrons being emitted. The secondary electrons ejected from the specimen surface are collected and displayed to provide a high-resolution micrograph. SEM sample preparation involves fixation (if proteins, cells, or tissue are present), followed by drying, attachment to a metallic stub, and then coating with a metal prior to data collection. In addition to imaging the surface morphology of polymeric biomaterials, the SEM can be combined with other analytical methods such as EDS to determine elemental distribution and composition (Sodhi, 1996). Viewing 3D images of microscopic areas only solves half the problem in an analysis. It is sometime necessary to identify the different elements associated with a specimen. This can be done by using the "built-in" spectrometer called an EDS. EDS utilizes X-rays that are emitted from the specimen when bombarded by the electron beam to identify the elemental composition of the specimen. When the sample is bombarded by the electron beam of the SEM, electrons are ejected from the atoms on the specimen's surface. A resulting electron vacancy is filled by an electron from a higher shell, and an X-ray is emitted to balance the energy difference between the two electrons.

The EDS X-ray detector measures the number of emitted X-rays versus their energy. The energy of the X-ray is characteristic of the element from which the X-ray was emitted. A spectrum of the energy versus relative counts of the detected X-rays is obtained and evaluated for qualitative and quantitative determinations of the elements present in the specimen.

3.1.2.2.4.2. Thermogravimetric analysis (TGA)

Thermogravimetric analysis or thermal gravimetric analysis (TGA) is a type of testing performed on samples that measures the weight loss of a material as a function of temperature in a controlled atmosphere (Gooch, 2010). TGA is commonly employed in research and testing to determine the characteristics such as degradation temperature and moisture content of polymer materials including EPS (Mishra et al., 2011). Analysis is carried out by increasing the temperature of the sample gradually and plotting weight (%) against temperature. Measurements are used primarily to determine the composition of polymers and to predict their thermal stability at temperatures up to 1000 °C.

3.1.2.2.4.3. Differential Scanning Calorimetry (DSC)

Differential Scanning Calorimetry measures the dissimilarity in heat flow between a sample and a reference as the material is heated or cooled. DSC instrument convert temperature differences into a measurement of the energy per unit mass related with the phase change that caused the temperature differences to arise. Any alteration in a material that involves a change in the heat content of the material can be detected and measured by DSC. These measurements provide quantitative and qualitative information

about physical and chemical changes that involve endothermic or exothermic processes, or differences in heat capacity. A primary use of DSC in polymer analysis is the detection and quantification of the crystalline melting process. Since the crystalline state in a polymer is influenced by inherent properties such as molecular weight distribution and the subsequent environmental treatment, this property is of considerable importance. Many polymers are unable to crystallize under normal condition and even semi-crystalline polymers contain a significant amount of material that remains in the amorphous state. Without crystals there can be no melting point; however the amorphous regions do undergo an important phase change known as the glass transition. The glass transition is defined as the beginning of conjugated main chain motion, a phenomenon where extended sections of individual chains become capable of independent motion. In amorphous polymers the glass transition indicates the softening of polymer. DSC detects the glass transition as a step change in the heat capacity of the polymer. Degradation is a catastrophic event and involves irreversible modification that can reduce the performance of a material. In semi-crystalline materials degradation can be detected by DSC as decrease in the melting and re-crystallization temperatures as well as the energy of these reactions.

3.1.2.2.4.4. Fourier transform infrared spectroscopy (FT-IR)

Infrared spectroscopy is a technique that measures the bond vibration frequencies in a molecule and can provide unique insights about the functional group within a molecule (Smith, 2011). The technique is relatively simple, reproducible, nondestructive, and only small amounts of material (micrograms to nanograms) with a minimum sample

preparation are required. FT-IR peaks are in many cases found associated with the vibration of a particular chemical bond (or a single functional group) in the molecule (Hofman et al., 2006). Due to the ability of infrared spectroscopy to identify the types and number of different chemical functional groups like hydroxyl, carboxyl, amino etc. present at a surface in a nondestructive manner, it has been widely used in the field of chemistry and biology. Many investigators have used FT-IR technique for the determination of functional groups in EPS (Yadav et al., 2012).

It is well documented that polysaccharides activate macrophages, T-helper, NK, and other effector cells and thereby activate the various cytokines (IL-2, IL-6, IL-10, and IL-12), interferon (IFN- γ), and chemokines which ultimately stimulate host's immune system. It has been observed that the molecular mass, degree of branching, conformation and chemical modification of polysaccharides significantly affect their anti-tumor and immunomodulatory activities (Bohn & BeMiller, 1995).

In this part of the work structural elucidation and immunogenic properties of the purified *K. pneumoniae* PB12 EPS has been presented following each of the analytical methodologies described in the preceding paragraphs.

3.2. Materials and methods

3.2.1. Functional group analysis

The functional group of EPS was determined by Fourier transform infrared (FT-IR) spectroscopy. Pellets of 2 mg of purified EPS were prepared with KBr followed by pressing the mixture into a 16 mm diameter mold. The infrared spectrum was recorded on

Perkin Elmer spectrum GX FT-IR system (PerkineElmer, USA) with resolution of 4 cm^{-1} in 4000-400 cm^{-1} region as described previously (Yadav et al., 2012).

3.2.2. Purification and chemical analysis of the polysaccharide fraction of Klebsiella pneumonaie EPS

Protein fraction of EPS was removed by adding trichloroacetic acid (30%) followed by centrifugation and residue was discarded. Two volumes of 95% ethanol was added to the supernatant and centrifuged at 9587.5 x *g* for 30 min to obtain 300 mg of protein-free crude polysaccharide (Zhang et al., 2002). This crude polysaccharide (25 mg) was passed through Sepharose 6B gel permeation column (90×2.1 cm) using water as the eluent with a flow rate of 0.3 ml min^{-1} as described in the earlier report (Davey & O'Toole, 2000). A total of 95 test tubes were collected using Redifrac fraction collector and monitored spectrophotometrically (Shimadzu UV-vis spectrophotometer, model-1601) at 490 nm using phenol-sulfuric acid method (York et al., 1986). Single fraction of purified polysaccharide (test tubes, 24-40) named KNPS was obtained.

3.2.3. General methods

The average molecular weight of KNPS was determined by gel chromatography using standard dextrans T-200, T-70 and T-40 as reported earlier (Sen et al., 2014). KNPS (2 mg) was hydrolyzed with 2 M CF_3COOH (2 ml) in a round-bottomed flask at 100 ºC for 18 h in a boiling water bath and the sugar composition analysis was carried out adopting the methods as described earlier (Sen et al., 2014). Gas Chromatography (GC) analysis of the alditol acetates was carried out by a gas-liquid chromatography, Hewlett-

Packard model 5730 A, with flame ionization detector and glass columns (1.8 m x 6 mm) packed with 3% ECNSS-M (A) on Gas Chrom Q (100-120 mesh) and 1% OV-225 (B) on Gas Chrom Q (100-120 mesh). All GC analyses were performed at 170 ºC. The absolute configuration of the monosaccharide was determined by the method of Gerwig et al. (1978). KNPS (3.5 mg) was methylated using the procedure reported earlier (Ciucanu & Kerek, 1984) and the partially methylated alditol acetates were analyzed by GC-MS. GC-MS analysis was performed on Shimadzu GC-MS Model QP-2010 Plus automatic system, using ZB-5MS capillary column (30 m x 0.25 mm). The program was isothermal at 150 ºC; hold time 5 min, with a temperature gradient of 2 ºC min^{-1} up to a final temperature of 200 ºC. NMR experiments were carried out by a Bruker Avance DPX-500 instrument at 30 °C as reported earlier (Sen et al., 2014).

3.2.4. Smith degradation study

KNPS (30 mg) was added to 7.5 ml 0.1 M sodium metaperiodate solution and the mixture was kept for 48 h in the dark at 4 °C. The excess periodate was destroyed by adding ethylene glycol (5.0 ml) and the solution was dialyzed against distilled water for 2 h. The volume of the dialyzed material was concentrated to 2–3 ml. This material was reduced with $NaBH_4$, 12 h, neutralized with 50% AcOH, and dialyzed with distilled water and finally freeze dried (14.0 mg). The periodate-oxidized, reduced material was subjected to mild hydrolysis by the addition of 0.5 M CF_3COOH for 15 h at 25 °C to destroy the residues of oxidized sugars attached to the polysaccharide backbone. The excess acid was removed by repeated freeze drying. The material was further purified by

passing through a Sephadex G-25 column, kept over P_2O_5 in vacuum for several days and finally used for ^{13}C NMR studies.

3.2.5. Biological activities

3.2.5.1. Isolation of lymphocytes from peripheral blood mononuclear cells (PBMCs)

Blood samples (total 30 blood samples, 6 samples for each group) were freshly collected satisfying the Helsinki protocol from all groups of individuals. From the heparinized blood samples the lymphocytes were isolated according to the method described earlier (Chattopadhyay et al., 2013). Blood was diluted in PBS (pH 7.0), layered carefully on the density gradient (histopaque 1077) in a ratio of 1:2, centrifuged at 1400 rpm for 20 min. The white milky layer of mononuclear cells were carefully removed and cultured in RPMI 1640 medium for 2 h under 5% CO_2 and 95% humidified atmosphere at 37 °C (Chattopadhyay et al., 2013). Non adherent layer of the cultured cells were collected and washed twice with PBS and centrifuged at 2000 rpm for 10 min to obtain lymphocytes. As described previously, the depletion of macrophages and B cells in PBMC were done by passing it through a nylon wool column (Saxena et al., 1980). After washing the column for two times with the medium, the non-adherent $CD4^+$ T cells and $CD8^+$ T cells were stained with Phycoerythrin (PE) and Fluorescein isothiocyanate (FITC) conjugated antibody as described earlier (Garcia et al., 2007). Samples were then analyzed using flow cytometer (FACS CALIBUR, Becton Dickinson, USA) using CellQuest software.

3.2.5.2. Sulforhodamine B assay (SRB)

The isolated human lymphocytes were seeded into 96 well tissue culture plates having 180 µl of complete media and were incubated for 48 h. KNPS was added to the cells at varied concentrations (25, 50, 100 and 200 µg $m1^{-1}$) and incubated for 24 h at 37 °C in a humidified incubator (NBS) containing 5% CO_2. The toxicity of KNPS on human lymphocytes were determined using SRB assay following the protocol described earlier (Vichai & Kirtikara, 2006).

3.2.5.3. Preparation of cell lysate

The cell suspension was centrifuged at 1500 rpm for 5 min, after treatment schedule. The supernatants were collected and stored at -20 °C. The cell pellets were re-suspended in ice cold PBS and subjected to four cycles of freeze-thaw cycles followed by sonication for 20 s (Ultrasonic Processor, Tekmar, Cincinnati, OH, USA). Lysates were centrifuged at 9587.5 x *g* for 20 min at 4 °C to remove cellular debris. Protein content of lysate was measured as described earlier using bovine serum albumin as standard (Lowry et al., 1951).

3.2.5.4. Determination of reduced glutathione (GSH), oxidized glutathione level (GSSG) and lipid peroxidation

The estimation of reduced glutathione in the cell lysate was done by the method described previously (Maity et al., 2014). The oxidized glutathione level was measured after derivatization of GSH with 2-vinylpyridine according to the method reported earlier

(Mahapatra et al., 2009). Lipid peroxidation was estimated using the method of Ohkawa et al. (1979) in the cell lysate.

3.2.6. Statistical analysis

The data were expressed as the mean ± the standard error of the mean (n = 6). Comparisons between the means of control and treated groups were made by one-way Anova analysis of variance (using a statistical package; Origin 6.1, Origin Lab, Northampton, MA, USA) with multiple-comparison tests, with $p<0.05$ as the limit of significance. The correlation analysis was performed using Statistica software version 8.0.

3.3. Results

3.3.1. Functional group determination, purification of polysaccharide fraction and chemical analysis of exopolysaccharide produced by K. pneumoniae PB12

FT-IR analysis showed the presence of hydroxyl (3384 cm^{-1}), weak C-H band at 2930 cm^{-1}, carboxyl (1616 cm^{-1} and 1408 cm^{-1}) and methoxyl (1077 cm^{-1}) groups (Fig. 3.1a). The isolation and purification steps are summarized in the flow diagram (Fig. 3.1b).

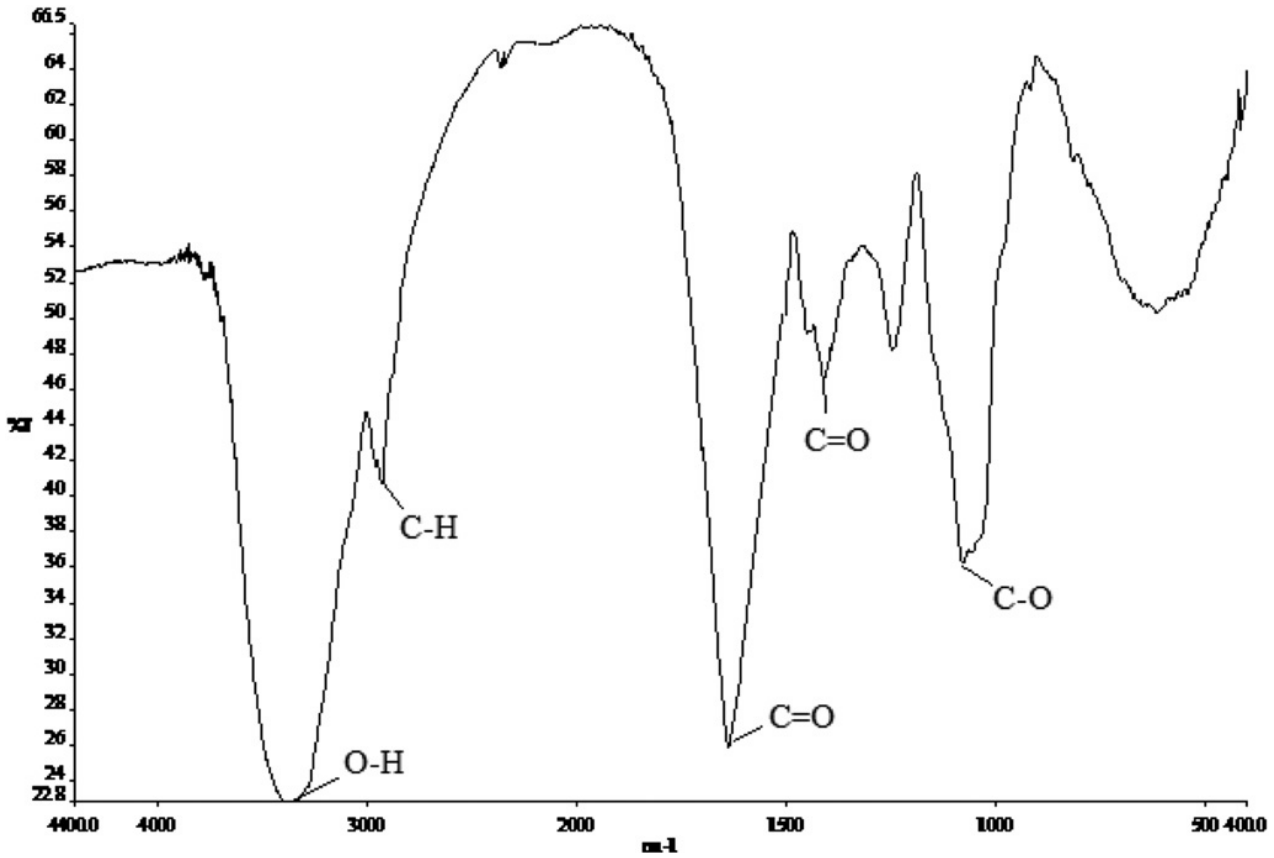

Fig. 3.1. a) FT-IR spectra of purified EPS.

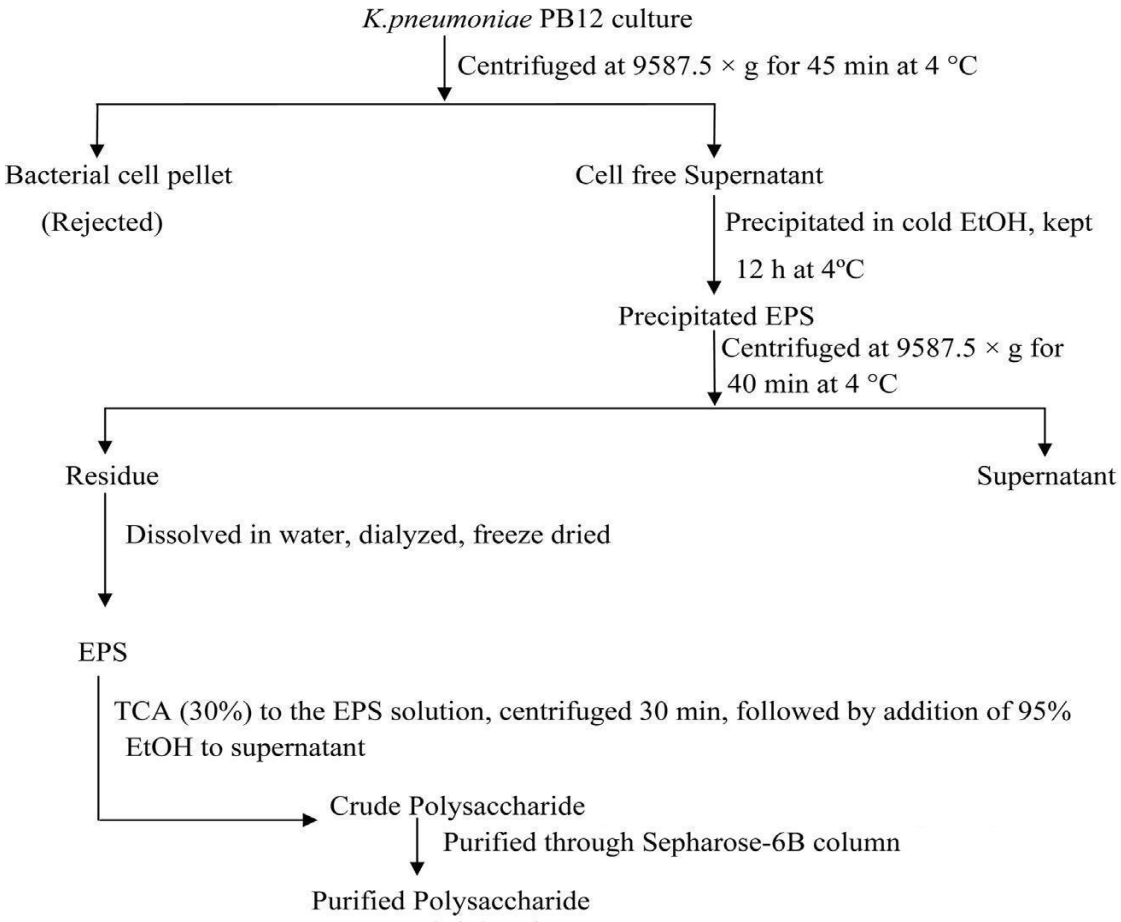

Fig. 3.1. b) Flow diagram of isolation and purification of the exopolysaccharide, KNPS produced by *K. pneumoniae* PB12.

A single fraction (Fig 3.2) of purified polysaccharide (KNPS) was obtained after fractionation of water soluble crude polysaccharide through Sepharose 6B column.

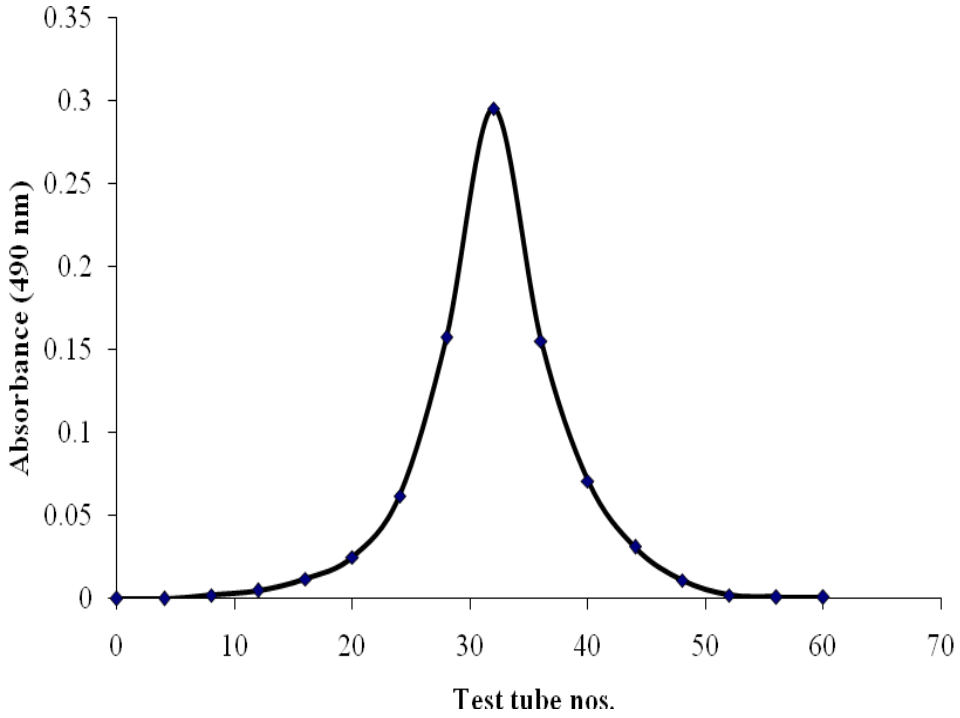

Fig. 3.2. Gel permeation chromatogram of crude exopolysaccharide isolated from the culture medium of *K. pneumoniae* PB12 using Sepharose 6B column.

The fraction was collected and freeze dried. KNPS was composed of arabinose, galactose, 3-*O*-methyl-galctose and glucose in a molar ratio of nearly 4:3:1:1. Determination of absolute configuration of the monosaccharides showed that galactose, 3-*O*-methyl-galctose and glucose were present in D and arabinose in L configuration. The GC–MS analysis of partially methylated alditol acetates revealed the presence of 3,5-linked-arabinofuranosyl, 2,6-linked-galactopyranosyl, 6-linked-galactopyranosyl, 6-linked-glucopyranosyl, 2-linked-galactopyranosyl, 5-linked-arabinofuranosyl, 3-linked-arbinopyranosyl, terminal galactopyranosyl and arabinofuranosyl residues in a relative proportion of approximately 1:1:1:1:1:1:1:1:1.

3.3.2. Structural analysis of KNPS

The ^{1}H NMR spectrum (500 MHz, Fig. 3.3) of KNPS recorded in D_2O at 30 ºC showed the presence of eight signals in the anomeric region at δ 5.20 (**A**), 5.17 (**B**), 5.16 (**C** and **D**), 5.10 (**E**), 5.05 (**F**), 5.02 (**G**), 4.46 (**H**), and 4.42 (**I**) as evidenced from HSQC couplings.

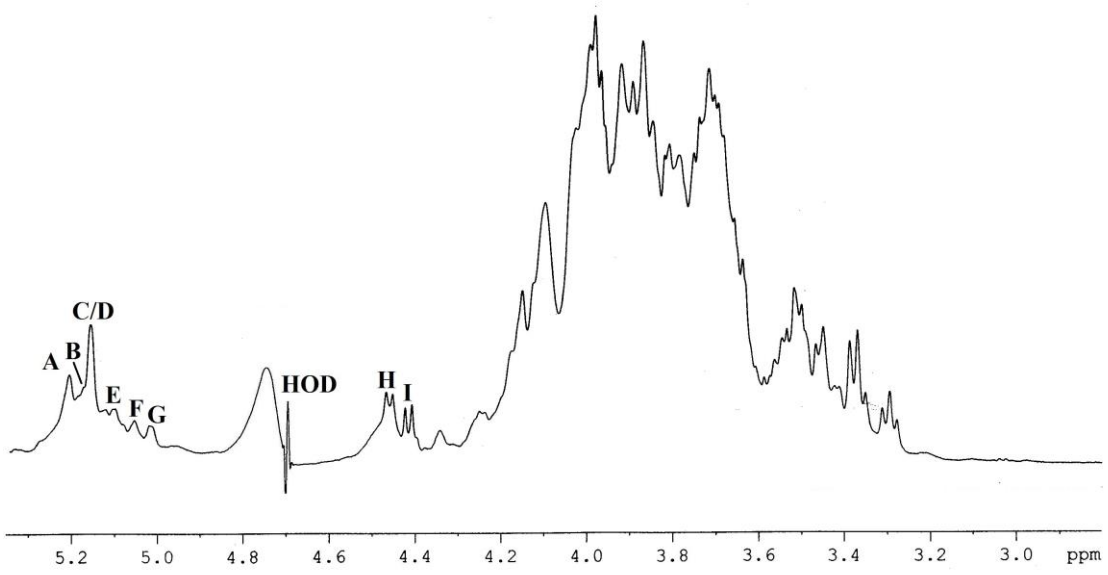

Fig. 3.3. ^{1}H NMR spectrum (500 MHz, D_2O, 30 ºC) of exopolysaccharide, KNPS produced by *K. pneumoniae* PB12. Acetone was taken as the internal standard, fixing the methyl proton signal at δ 2.225.

In ^{13}C NMR spectrum (125 MHz; Fig. 3.4) at the same temperature, eight signals were observed in the anomeric region at δ 109.4, 106.8, 103.3, 102.7, 102.2, 101.5, 99.5, and 97.7.

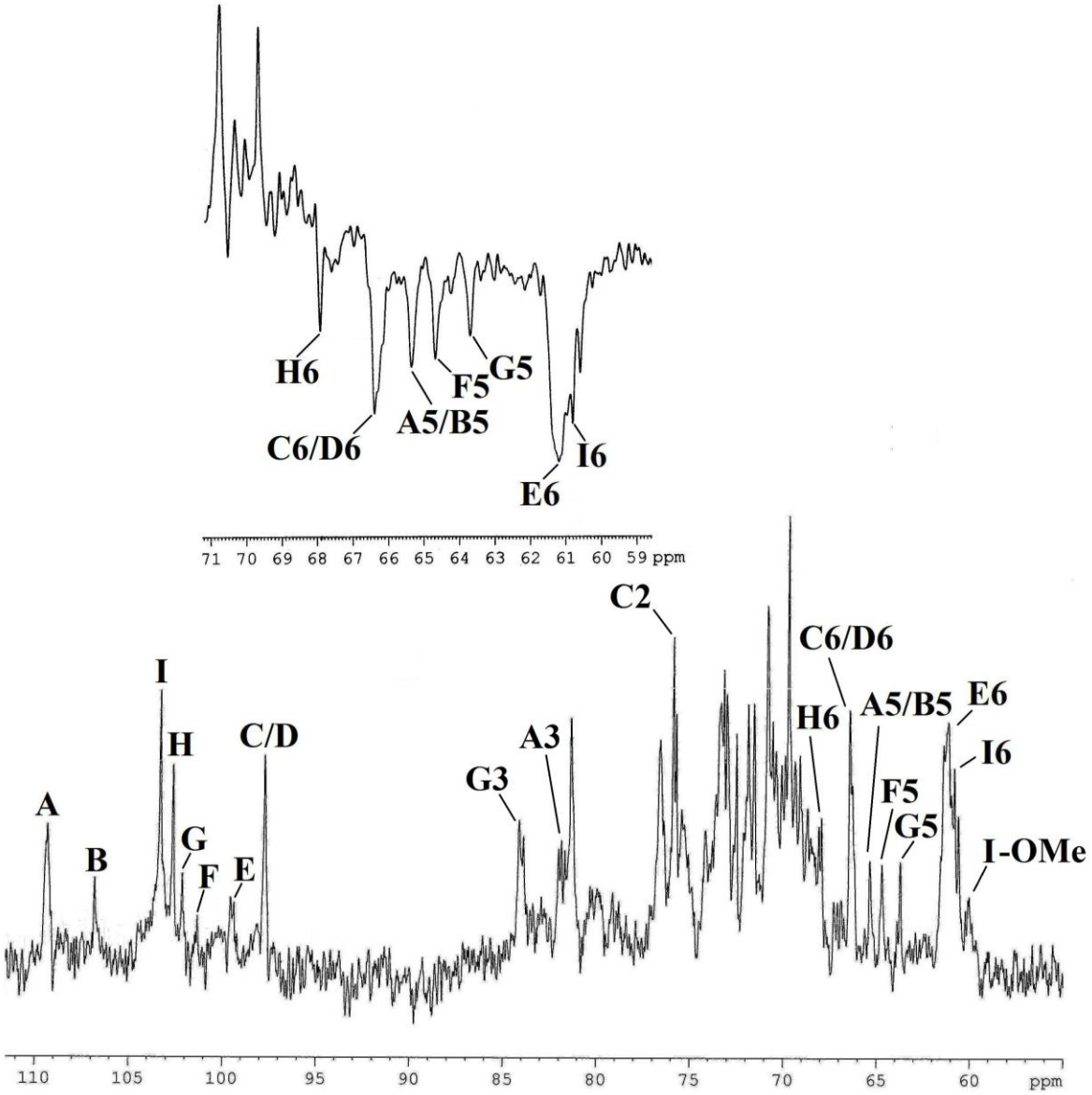

Fig. 3.4. ^{13}C NMR spectrum (125 MHz, D_2O, 30 ºC) of exopolysaccharide, KNPS produced by *K. pneumoniae* PB12, acetone was taken as the internal standard, fixing the methyl carbon signal at δ 31.05. Inset shows part of DEPT-135 spectrum (D_2O, 30 ºC) of exopolysaccharide, KNPS.

These eight anomeric carbon signals were correlated to the anomeric proton signals of residue (**A**), (**B**), (**I**), (**H**), (**G**), (**F**), (**E**), (**C** and **D**), respectively as assigned from the HSQC spectrum (Fig. 3.5a, Table 3.1).

The proton and carbon chemical shifts were assigned from DQF-COSY, TOCSY, and HSQC [Fig. 3.5a & 3.5 b] experiments. The proton coupling constants were measured from DQF-COSY experiment.

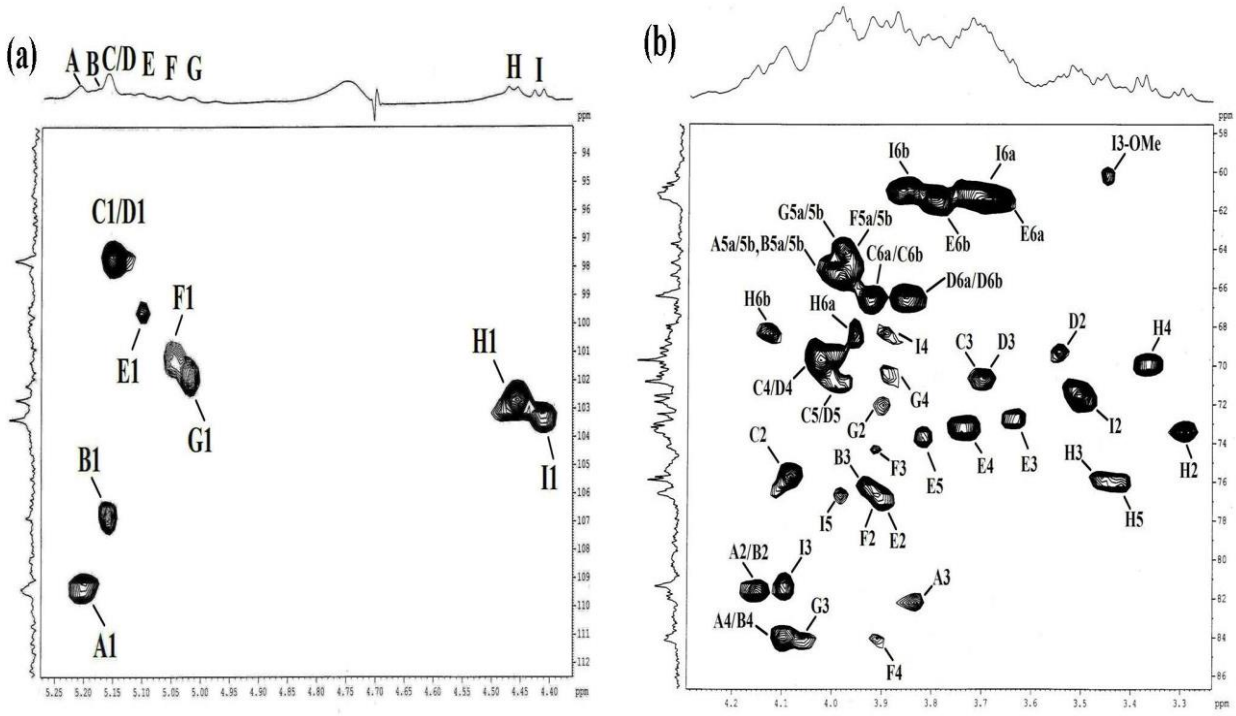

Fig. 3.5. The HSQC spectrum of **a**) anomeric part and **b**) other than anomeric part of the exopolysaccharide, KNPS produced by *K. pneumoniae* PB12. The annotation **A**1 refers to **A**H1/**A**C1 cross peak, **B**1 refers to **B**H1/**B**C1 cross peak and so on.

Table 3.1

The ^{1}H NMR[a] and ^{13}C NMR[b] chemical shifts of the exopolysaccharide, KNPS produced by *K. pneumoniae* PB12 in D_2O at 30 ºC.

Glycosyl residue	H-1/C-1	H-2/C-2	H-3/C-3	H-4/C-4	H-5a, H-5b/C-5	H-6a, H-6b/C-6	*O*Me
→3,5)-α-L-Ara*f*-(1→ **A**	5.20 109.4	4.15 81.5	3.85 81.8	4.09 84.0	3.98[c], 3.98[d] 65.4		
→5)-α-L-Ara*f*-(1→ **B**	5.17 106.8	4.15 81.4	3.92 76.6	4.09 84.0	3.98[c], 3.98[d] 65.4		
→2,6)-α-D-Gal*p*-(1→ **C**	5.16 97.7	4.09 75.9	3.70 70.8	4.02 69.7	3.99 70.8	3.92[c], 3.92[d] 66.4	3.45 59.9
→6)-α-D-Gal*p*-(1→ **D**	5.16 97.7	3.55 69.3	3.70 70.8	4.02 69.7	3.99 70.8	3.84[c], 3.84[d] 66.4	
→2)-α-D-Gal*p*-(1→ **E**	5.10 99.5	3.92 76.6	3.63 72.5	3.74 72.6	3.81 73.4	3.69[c], 3.78[d] 61.1	
β-L-Ara*f*-(1→ **F**	5.05 101.5	3.92 76.6	3.91 74.1	3.90 84.1	3.97[c], 3.97[d] 64.7		
→3)-β-L-Ara*p*-(1→ **G**	5.02 102.2	3.89 71.9	4.09 84.1	3.88 70.8	3.98[c], 3.98[d] 63.7		
→6)-β-D-Glc*p*-(1→ **H**	4.46 102.7	3.30 73.2	4.46 75.7	3.38 69.8	3.42 75.9	3.95[c], 4.13[d] 67.9	
3-*O*-Me-β-D-Gal*p*-(1→ **I**	4.42 103.3	3.50 70.8	4.09 81.4	3.89 68.0	3.98 76.6	3.70[c], 3.87[d] 60.8	

[a] Values of the ^{1}H chemical shifts were recorded with respect to the HOD signal fixed at δ 4.70 at 30 °C.

[b] Values of the ^{13}C chemical shifts were recorded with reference to acetone as the internal standard and fixed at δ 31.05 at 30 °C.

[c,d] Interchangeable.

The residues **A** and **B** were assigned as (1→3,5)-α-L-Ara*f* and (1→5)-α-L-Ara*f* residues respectively. The α-configuration of both **A** and **B** residues were assigned from the chemical shift values of anomeric carbon and proton (δ 109.4/5.20 and δ 106.8/5.17) respectively. The downfield shift of C-3 (δ 81.8) and C-5 (δ 65.4) with respect to the standard methyl glycosides (Rinaudo & Vincendon, 1982; Agarwal, 1992; Mandal et al., 2011) indicated that the residue **A** was (1→3,5)-linked-α-L-arabinofuranose. The downfield shift of C-5 (δ 65.4) with respect to the standard methyl glycosides indicated that the residue **B** was (1→5)-linked α-L-arabinofuranosyl moiety. The linkage at C-5 of the both residues **A** and **B** were further confirmed from DEPT-135 spectrum (Fig. 3.4 inset). Hence, these observation confirmed that the residue **A** was (1→3,5)-α-L-Ara*f* and the residue **B** was (1→5)-α-L-Ara*f*.

The anomeric proton chemical shifts (δ 5.16 for **C** and **D,** δ 5.10 for **E**) and carbon chemical shifts (δ 97.7 for **C** and **D,** δ 99.5 for **E**) confirmed that the residues were α-D-galactopyranosyl residues. In case of residue **C**, the carbon chemical shifts of C-2 (δ 75.9) and C-6 (δ 66.4) appeared at downfield with respect to the standard values of methyl glycosides (Rinaudo & Vincendon, 1982; Agarwal, 1992) which suggests that residue **C** was linked at C-2 and C-6. The linkage at C-6 of the residue **C** was further confirmed from DEPT-135 spectrum (Fig. 3.4 inset). Hence, **C** was confirmed as (1,2→6)-linked α-D-galactopyranosyl residue. Residue **D** had an anomeric carbon signal at δ 97.7. The downfield shift of C-6 (δ 66.4) of residue **D** with respect to standard methyl glycosides indicated that it was linked at C-6. The linkage at C-6 was further supported by DEPT-135 spectrum (Fig. 3.4 inset). Therefore, **D** was confirmed as (1→6)-

linked α-D-galactopyranosyl residue. The downfield shift of C-2 (δ 76.6) with respect to standard values of methyl glycosides (Rinaudo & Vincendon, 1982; Agarwal, 1992) indicated that residue **E** was a (1→2)-linked α-D-galactopyranosyl.

Residue **F** was assigned as non reducing end β-L-Ara*f*. The anomeric proton chemical shift for residue **F** at δ 5.05 and carbon chemical shift of δ 101.5 indicated that it was a β-linked anomer (Agarwal, 1992; Das et al., 2013).

The residue **G** was assigned as (1→3)-β-L-Ara*p*. The anomeric proton (δ 5.02) and carbon (δ 102.2) chemical shift values indicated that **G** was a β-linked anomer. The downfield shift of C-3 at δ 84.1 indicated that it was (1→3)-β-L-Ara*p* (Chandra et al., 2009).

Anomeric proton chemical shift (δ 4.46), anomeric carbon chemical shift (δ 102.7), and the coupling constant value $J_{H\text{-}1,H\text{-}2}$ (~8.0 Hz) confirmed that **H** was β-D-glucopyranosyl residue. The downfield shifts of C-6 (δ 67.9) with respect to standard values of methyl glycosides indicated that residue **H** was linked at this position. The linking at C-6 of the residue **H** was further confirmed by DEPT-135 spectrum (inset, Fig. 3D). Thus, **H** was confirmed as (1→6)-β-D-glucopyranosyl residue.

β-configuration of residue **I** was assigned from $J_{H\text{-}1,H\text{-}2}$ coupling constant (~8.5 Hz) from its anomeric proton (δ 4.42) and carbon (δ 103.3) signals. All the proton and carbon chemical signals except C-3 matched nearly to the standard values of methyl glycosides (Rinaudo & Vincendon, 1982; Agarwal, 1992). The ^{13}C chemical shift of C-3 is about ~δ 10.0 higher than the standard value (Agarwal, 1992; Popper et al., 2001) which is consistent with the presence of -*O*Me group at C-3. This was further confirmed by the presence of cross coupling between the methoxy proton (δ 3.45) and the C-3 (δ

81.4) of residue **I** in the HMBC experiment (Figure not shown). Thus, **I** was confirmed as terminal 3-*O*-methyl-β-D-galactopyranosyl residue.

The sequence of glycosyl residues (**A** to **I**) were determined from ROESY (Table 3.2, Fig. 3.6) experiment.

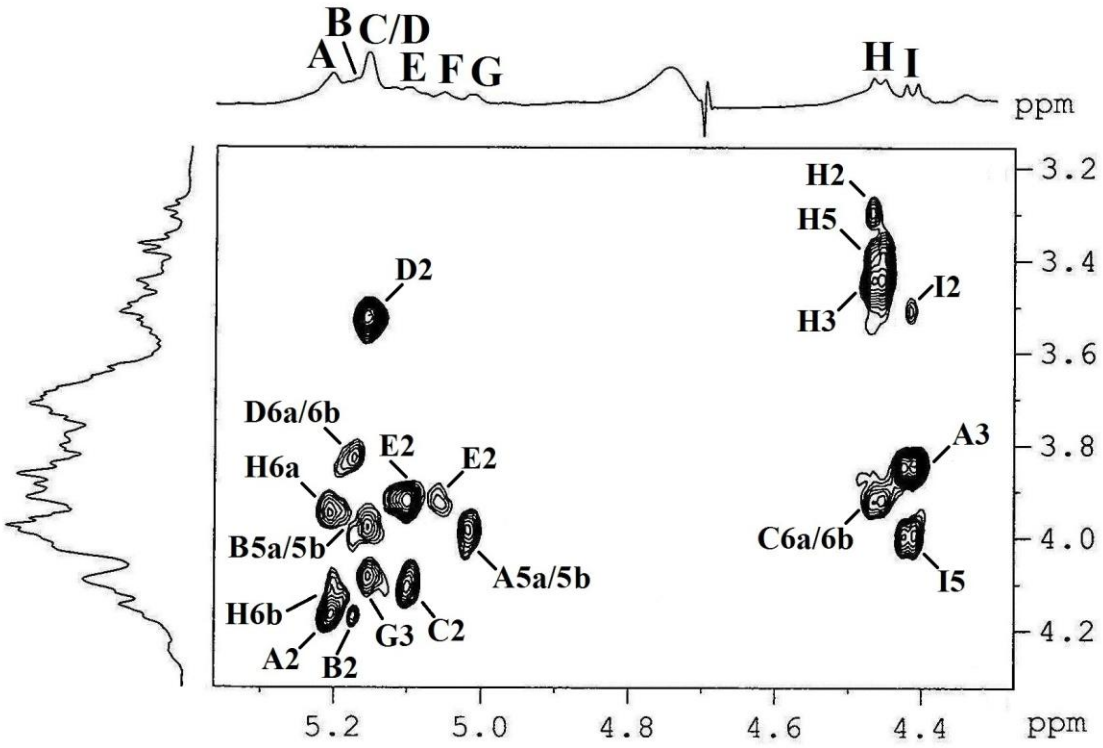

Fig. 3.6. Part of ROESY spectrum of exopolysaccharide, KNPS produced by *K. pneumoniae* PB12. The ROESY mixing time was 300 ms.

Table 3.2

ROESY data of exopolysaccharide, KNPS produced by *K. pneumoniae* PB12 in D_2O at 30 ºC.

Glycosyl residue	Anomeric proton	ROE contact protons	
	δ	δ	Residue, atom
→3,5)-α-L-Ara*f*-(1→ **A**	5.20	3.95	**H** H-6a
		4.13	**H** H-6b
		4.15	**A** H-2
→5)-α-L-Ara*f*-(1→ **B**	5.17	3.84	**D** H-6a/b
		4.15	**B** H-2
→2,6)-α-D-Gal*p*-(1→ **C**	5.16	3.98	**B** H-5a/b
		4.09	**G** H-3
→6)-α-D-Gal*p*-(1→ **D**	5.16	3.55	**D** H-2
		4.09	**C** H-2
→2)-α-D-Gal*p*-(1→ **E**	5.10	3.92	**E** H-2
		3.92	**E** H-2
β-L-Ara*f*-(1→ **F**	5.05	3.98	**A** H-5a/b
		3.92	**C** H-6a/b
→3)-β-L-Ara*p*-(1→ **G**	5.02	3.30	**H** H-2
		3.46	**H** H-3
→6)-β-D-Glc*p*-(1→ **H**	4.46	3.42	**H** H-5
		3.85	**A** H-3
3-*O*-Me-β-D-Gal*p*-(1→ **I**	4.42	3.98	**I** H-5
		3.50	**I** H-2

In ROESY experiment, the inter-residual contacts **A**H-1/**H**H-6a, 6b; **B**H-1/**D**H-6a, 6b; **C**H-1/**B**H-5a, 5b; **D**H-1/**G**H-3; **E**H-1/**C**H-2; **F**H-1/**E**H-2; **G**H-1/**A**H-5a, 5b; **H**H-1/**C**H-6a, 6b; and **I**H-1/**A**H-3 along with other intra-residual contacts were also observed (Fig. 3.6). The above ROESY connectivities established the following sequences: **A** (1→6) **H; B** (1→6) **D; C** (1→5) **B**; **D** (1→3) **G; E** (1→2) **C; F** (1→2) **E**; **G** (1→5) **A**; **H** (1→6) **C**; and **I** (1→3) **A**. Hence, the structure of repeating unit present in KNPS was proposed as:

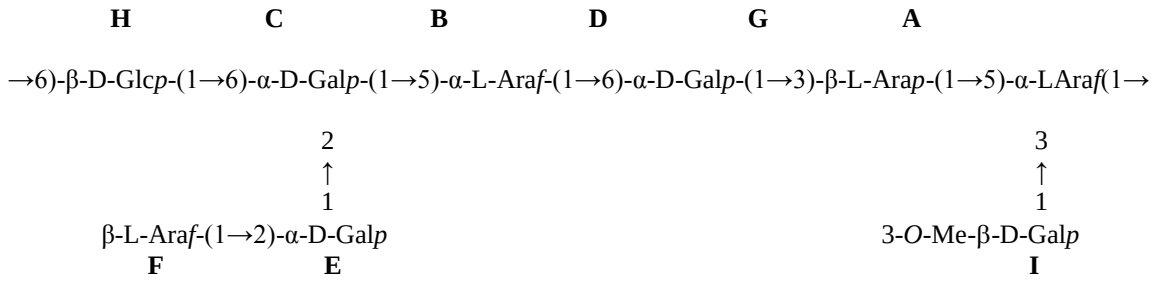

3.3.3. Smith degradation study

Smith degradation was carried out with KNPS and the product was analyzed by ^{13}C NMR (Table 3.3, Fig. 3.7) to confirm the sequence of the sugar residues present in the repeating unit.

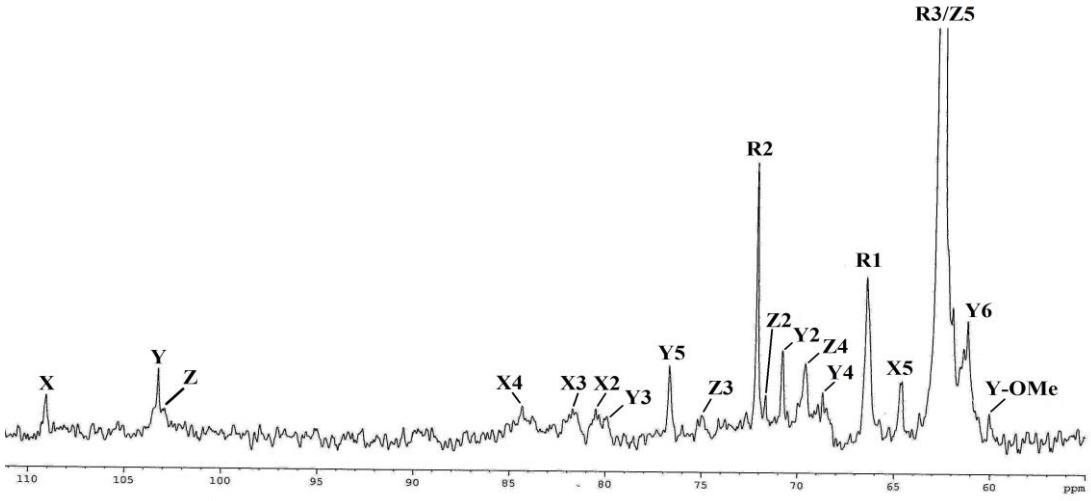

Fig. 3.7. ^{13}C NMR spectrum (125 MHz, D_2O, 30 ºC) of glycerol containing trisaccharide residue obtained from Smith-degradation of KNPS produced by *K. pneumoniae* PB12.

Table 3.3.

The ^{13}C NMR[n] chemical shifts of trisaccharide unit obtained after Smith-degradation of exopolysaccharide, KNPS produced by *K. pneumoniae* PB12 in D_2O at 30 ºC.

Sugar residue	C-1	C-2	C-3	C-4	C-5	C-6	*O*Me
→3,5)-α-L-Ara*f*-(1→ **X**	109.2	80.2	81.5	84.0	64.6	-	
3-*O*-Me-β-D-Gal*p*-(1→ **Y**	103.2	70.8	79.8	68.8	76.7	61.2	60.0
β-L-Ara*p*-(1→ **Z**	102.9	71.8	74.9	69.6	63.0	-	
1 2 3 (CH$_2$OH) CH(OH) CH$_2$O→ **R**	66.4	72.1	62.6	-	-	-	

[n] Values of the ^{13}C chemical shifts were recorded with reference to acetone, fixing the methyl carbon signal at δ 31.05.

A trisaccharide containing glycerol moiety was obtained as a product of Smith degradation of KNPS. The ^{13}C NMR spectrum of Smith-degraded KNPS showed three anomeric signals at δ 109.2, 103.3 and 102.9 corresponding to the anomeric carbon of →3,5)-α-L-Ara*f*-(1→ residue (**X**), 3-*O*-Me-β-D-Gal*p*-(1→ residue (**Y**) and β-L-Ara*p*-(1→ moiety (**Z**), respectively. The carbon signal at δ 64.6 and δ 81.5 clearly indicated the presence of linking at C-5 and C-3 of →3,5)-α-L-Ara*f*-(1→ residue (**X**). The residue (**A**) of KNPS being (1→3,5)-linked remains unaffected during oxidation and assigned as residue (**X**) in the degraded product. The →3)-β-L-Ara*p*-(1→ residue (**G**) was converted to nonreducing end β-L-Ara*p*-(1→ (**Z**) during Smith degradation. The glycerol moiety (**R**) was generated from the (1→6)-β-D-Glc*p* moiety (**H**) which was linked glycosidically with the residue (**C**) in KNPS and remains attached to the →3,5)-α-L-Ara*f*-(1→ moiety (**X**) in the Smith degraded product. The residue 3-*O*-Me-β-D-Gal*p*-(1→, (**I**) remains unaffected during Smith degradation and assisgned as residue (**Y**) in the degraded product. The remaining residues **B**, **C**, **D**, **E**, **F** of KNPS were completely destroyed during oxidation. Hence, the structure of glycerol containing trisaccharide unit obtained from exopolysaccharide, KNPS after Smith degradation was established as:

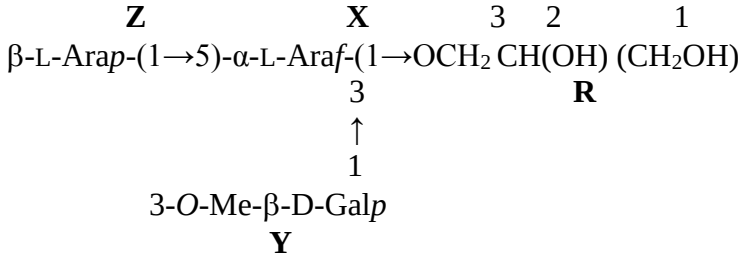

Therefore, Smith degradation results further confirmed the repeating unit present in the exopolysaccharide, KNPS produced by *K. pneumoniae* PB12.

3.3.4. Biological activities

The phenotypic characteristics of lymphocytes were confirmed by FACS analysis. The dot plot results showed that, 48% lymphocyte cells were $CD4^+$ and 23% $CD8^+$ [Fig. 3.8a]. The viability of the human lymphocytes was studied using SRB assay with varied concentrations of KNPS (ranging from 25-200 µg ml^{-1}) [Fig. 3.8b]. SRB, a bright pink aminoxanthene dye binds under mild acidic conditions to basic amino acid residues and dissociates under basic conditions. In order to understand the glutathione level, an important antioxidant in cellular system, both the reduced and oxidized form of glutathione were measured. It was observed that there was decrease in reduced glutathione (GSH) level at the dosage of 200 µg $m1^{-1}$ of KNPS whereas the same dosage of KNPS showed a mild increment of oxidized glutathione level (GSSG) ($p< 0.05$) [Fig. 3.8c]. Thus, it can be said that there is some relation between the redox ratios (GSH/GSSG) in cellular system with the concentration of KNPS used. Lipid peroxidation is one of the essential determinants to assess the cellular damage due to ROS. Several toxic by-products especially malondialdehyde (MDA) is released due to lipid peroxidation (Wood et al., 2003). Hence, the concentration of malondialdehyde (MDA) was measured to check the involvement of ROS in the alteration of redox status [Fig. 3.8d]. To further validate our observations, intracellular ROS was measured using a oxidant-sensing fluorescent probe 2',7'-dichlorodihydrofluorescein diacetate ($DCFH_2$-DA). $DCFH_2$-DA, a nonpolar dye, converted into the polar derivative DCFH (nonfluorescent) by means of cellular esterase. After getting oxidized by intracellular ROS and other peroxides it switched to highly fluorescent DCF. Fig. 3.8e, showed that

fluorescence intensity of DCF increase with the increment of KNPS dosage (varied between 25-200 µg $m1^{-1}$) and it becomes maximum at 200 µg $m1^{-1}$ (Fig.3.9.).

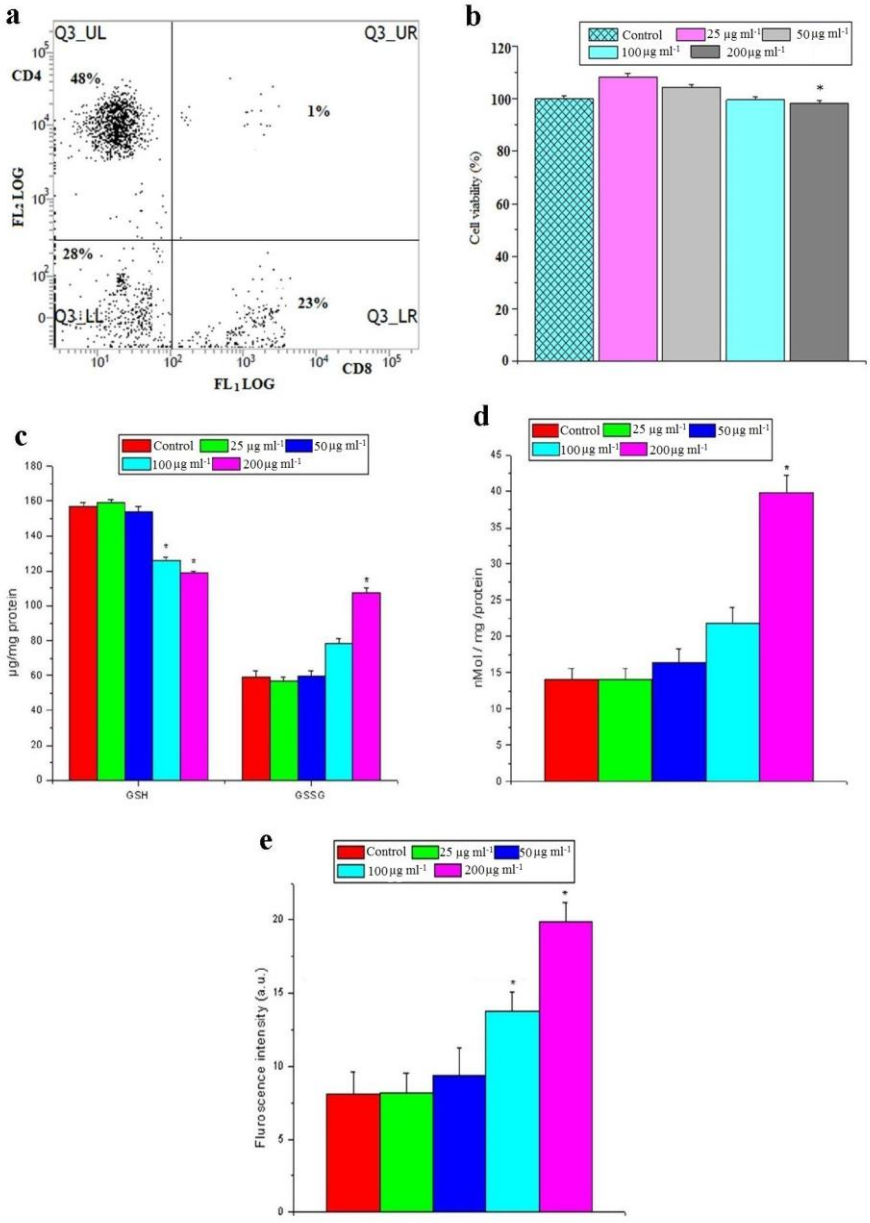

Fig. 3.8. a) Dot plot of lymphocytes stained with anti-CD4 or anti-CD8 antibodies. b) Cytotoxicity of KNPS against human lymphocytes. c) Concentration of reduced glutathione (GSH) and oxidized glutathione (GSSG) of normal human lymphocytes when

treated with KNPS. d) Lipid peroxidation study in terms of MDA release in KNPS treated human lymphocytes. e) Measurement of intracellular ROS in lymphocytes, using a oxidant-sensing fluorescent probe 2',7'-dichlorodihydrofluorescein diacetate (DCFH-DA), treated with varied concentration of KNPS. (n = 6, values are expressed as mean ± SEM. * Indicates the significant difference as compared to control group).

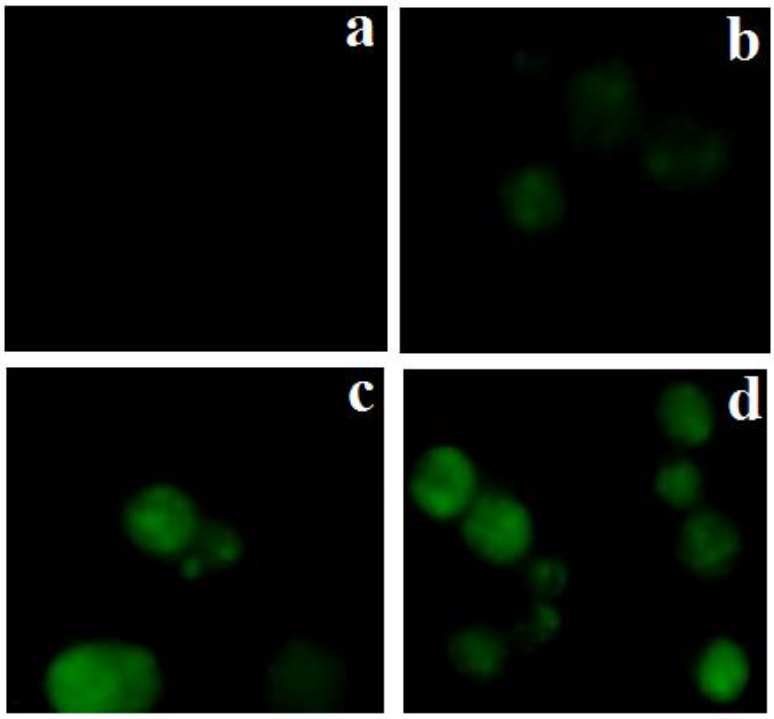

Fig. 3.9. Fluorescence micrographs of human lymphocytes treated with different concentrations of KNPS. a) Control, b) 50 µg $m1^{-1}$, c) 100 µg $m1^{-1}$ and d) 200 µg $m1^{-1}$.

3.4. Discussion

The average molecular weight of KNPS was estimated ~1.8×10^5 Da. Results obtained from biological studies showed that 200 µg $m1^{-1}$ dosage of KNPS exhibited toxicity ($p< 0.05$) (Fig. 3.9). Previous report established the potent role of *K. pneumoniae* CPS in initiation of cytotoxicity during the infection of lung epithelial cells (Cano et al., 2009). The increasing GSSG level may be due to the generation of free singlet species inside the cells. When the dose of the KNPS was increased from 25 to 200 µg $m1^{-1}$, the redox ratio decreased significantly ($p < 0.05$) to 1.11 compared to their respective control (redox ratio 2.66) indicating that 200 µg $m1^{-1}$ of KNPS was toxic. The significantly ($p< 0.05$) enhanced production of MDA was noted at 200 µg $m1^{-1}$ of KNPS dosage, which confirms the potential of KNPS to alter the intracellular redox status via ROS production. Similar type of enhanced ROS generation was reported in macrophage cell lines by the polysaccharide, PSG-1 (Yu et al., 2014). These results showed that KNPS treatment enhanced the generation of intracellular reactive oxygen species (ROS). It was reported earlier that the CPS of *K. pneumoniae* induce ROS production in macrophages (Yang et al., 2011). Hence, this study may help to put on more insights into the mechanisms of septic shock and KNPS-induced immunosuppression and autoimmunity.